FACULTY OF ENGINEERING SCIENCE
DEPARTMENT OF MECHANICAL ENGINEERING

Control Theory: Assignment 3: State feedback and state estimation

Maxime Brion (r0891121)
Mauro Van Tichelen (r0902198)

Professor: Prof. Swevers Jan

2024 - 2025

Contents

List of Figures

1 State Estimator and Feedback Controller Design

1a Discrete State Equation with Forward Euler Method

The system dynamics are modeled in discrete time, with the cart's angular velocity serving as the input. In this context, $u(t)$ denotes the input, r represents the radius, and x corresponds to the horizontal displacement. The modeling begins from the continuous-time state equation:

$$\dot{x} = u(t) \cdot r \tag{1}$$

The Forward Euler method was employed to discretize the equation:

$$\frac{x_{k+1} - x_k}{T_s} = ur \iff x_{k+1} = x_k + T_s \cdot u \cdot r \tag{2}$$

The state-space representation of the system is given by:

$$x_{k+1} = Ax_k + Bu_k \tag{3}$$

where:

$$A = [1], \quad B = [T_s r] \tag{4}$$

1b Measurement Equation

In discrete-time linear time-invariant (LTI) state-space representation, the measurement equation can be expressed as:

$$y(k) = Cx(k) + Du(k) \tag{5}$$

Since the distance to the wall x lies on the negative x-axis, [C] = [-1] such that the measured distance is positive. Since the measured distance is independent of the input u_k, [D] = 0.

1c State Feedback Controller Gain K Design

To determine the expression for the pole of the closed-loop system, the transfer function

$$H(z) = \frac{Y(z)}{R(z)} \tag{6}$$

is first derived. This process utilizes the relationships from the block diagram shown in Figure 1 and is detailed in equations 7 and 8.

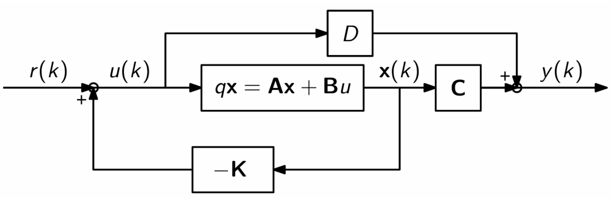

Figure 1: Full State Feedback

$$\begin{aligned} R(z) &= U(z) + KY(z) \\ &= B^{-1}(zI - A)X(z) + KY(z) \\ &= \frac{zI - A + KB}{CB} Y(z) \end{aligned} \tag{7}$$

$$H(z) = \frac{Y(z)}{R(z)} = \frac{CB}{zI - A + KB} \tag{8}$$

The system's pole corresponds to the root of the denominator. It can be determined as demonstrated in Equation 9.

$$\begin{aligned} zI &= A - KB \\ &= 1 - T_s r K \end{aligned} \tag{9}$$

The system will be considered stable if the pole lies within the unit circle.

$$|z| \leq 1 \tag{10}$$

This defines a restricted interval for the K value. If K falls outside this range, the pole will be positioned outside the unit circle, causing the system to become unstable.

$$0 < K < \frac{2}{T_s r} \tag{11}$$

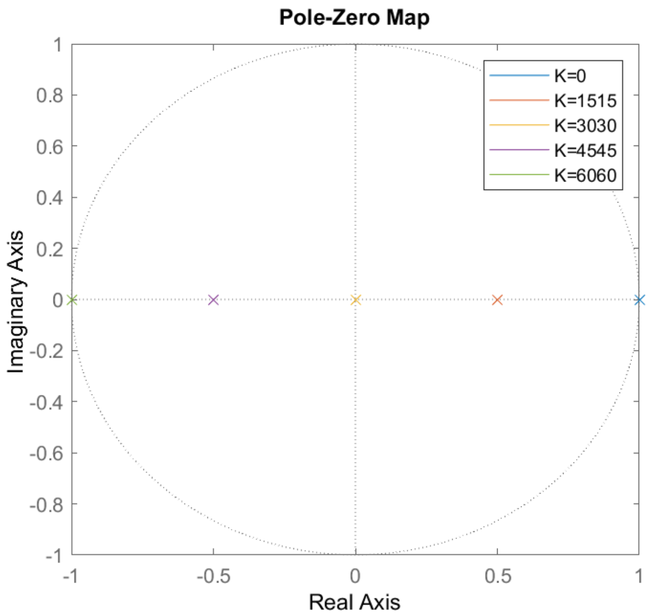

Figure 2: Influence of K on pole location

Next, we create a pole-zero map and illustrate how the pole locations change with varying values K values, as shown in Figure 2. Therefore, K influences the pole placement, which in turn affects the system's stability. In this system, a sampling time of $T_s = 0.01\,\mathrm{s}$ and a radius of $r = 0.033\,\mathrm{m}$ are used. According to Equation 11, $K \in [0, 6060]$.

The closed loop step response is shown in Figure 3. $K = 0$ms and $K = 6060$ms are left out since these are unstable. Note that the value for K that corresponds with a pole close to the origin has the best damping behavior. Increasing or decreasing K, corresponds with a slower transient. Thus $K = 3030$ ms is preferred.

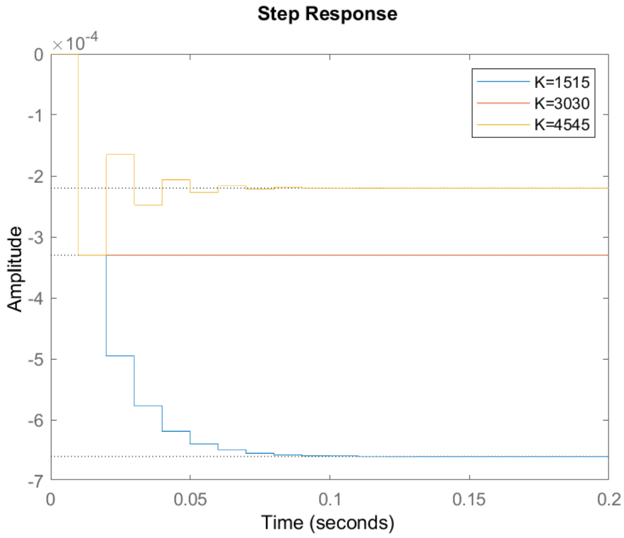

Figure 3: Closed loop step response for varying K

1d State Estimator Gain L Design

To derive the expression for the pole of the closed-loop system, we refer to the block diagram in Figure 4.

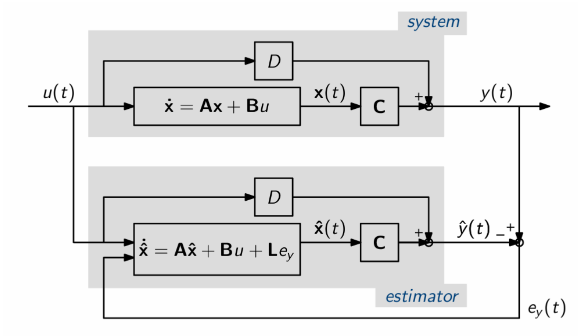

Figure 4: Closed Loop State Estimator

The closed-loop estimator dynamics are described by:

$$\dot{e}_x(t) = (A - LC)e_x(t) \tag{12}$$

where L is the estimator gain, A is the system matrix, and C is the output matrix. In discrete time, with sample time T_s, the continuous poles p_c of the matrix $A - LC$ are mapped to discrete poles p_d as:

$$p_d = e^{T_s p_c} \tag{13}$$

Here, p_c represents the eigenvalues of $A - LC$, which are directly influenced by the choice of L.

The effect of L is straightforward: increasing L moves the eigenvalues of $A - LC$ further to the left in the s-plane, resulting in faster estimator dynamics. In the discrete domain, this causes the poles p_d to move closer to the origin. However, if L is chosen poorly, the eigenvalues of $A - LC$ may acquire positive real parts, leading to instability. In discrete time, this instability manifests as poles p_d lying outside the unit circle, violating stability conditions.

When designing the gain L, the estimator poles are typically placed 2 to 6 times faster than the controller poles. This ensures that estimation errors decay quickly without interfering with the control dynamics. However, this design introduces a trade-off:

- faster poles provide rapid convergence but amplify measurement noise.
- Slower poles reduce noise sensitivity but introduce delays in the state estimation.

The goal is to achieve a balance between estimation speed and noise sensitivity. By carefully tuning L and ensuring the estimator poles remain inside the unit circle in the z-domain, a stable and accurate estimator can be designed that meets performance specifications.

To balance the trade-off between convergence speed and noise sensitivity, the estimator poles were selected to be four times faster than the controller poles. This design choice resulted in an estimator gain of $L = -0.1681$. Notably, L is dimensionless.

2 State Estimator and Feedback Controller Implementation

2a State Estimator Testing with Initial Estimation Error

From Figure 5, it can be observed that the estimates converge progressively faster to the measurements as the estimator poles are placed further to the left (or closer to the origin in the discrete domain). Specifically:

- For 2x faster poles ($L = -0.0879$), the convergence is relatively smooth and already quite fast.
- For 4x faster poles ($L = -0.1681$), the convergence improves slightly, achieving faster estimation without significant changes in overall behavior.
- For 6x faster poles ($L = -0.2412$), the convergence is marginally faster, but the improvement is less pronounced compared to the jump from 2x to 4x.

While the differences in convergence speed between 2x, 4x, and 6x are subtle, the general trend confirms that larger absolute values of L result in slightly faster convergence. However, this comes with the trade-off of increased sensitivity to noise, which becomes more noticeable as L increases.

Overall, 4x faster poles ($L = -0.1681$) provide a good balance, delivering a slight improvement in convergence speed over 2x.

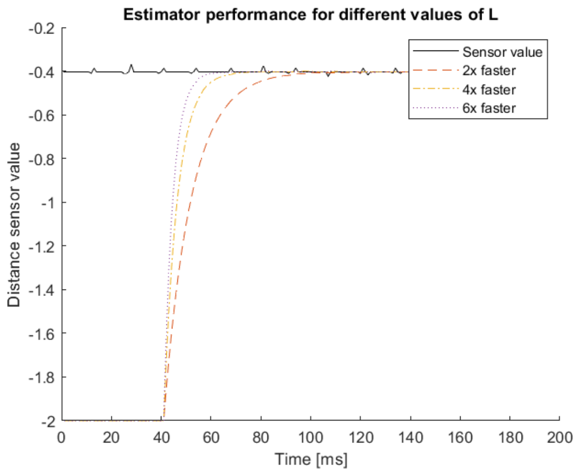

Figure 5: Convergence of estimates to the measurements

2b Step Response and Control Signals with Proportional Controller for Different K Values

As detailed in Section 1c, the system's response speed is closely tied to the location of the poles in its transfer function. Poles positioned nearer to the origin result in faster system responses, with a pole exactly at the origin theoretically corresponding to a controller gain of $K \approx 3030$. Figure 2 illustrates that increasing K shifts the poles closer to the origin, thereby accelerating the system's convergence. However, higher K values require greater voltage, introducing a trade-off between improved responsiveness and practical voltage constraints.

Experimental observations reveal that implementing very large K values, such as $K = 3030$, is not feasible in practice due to physical limitations on the voltage supply. Consequently, lower K values were explored. Figure 6 shows the step responses for various K values, demonstrating that $K = 10$ leads to an unacceptably slow response. In contrast, both $K = 50$ and $K = 100$ achieve fast and stable step responses, making them more suitable for practical application.

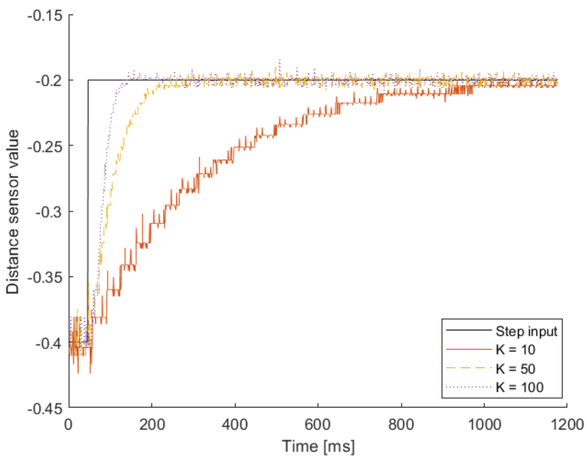

Figure 6: Step response for different values of K

The controller gain K scales the error signal, defined as the difference between the reference position and the measured position, to compute the desired velocity. This desired velocity determines the velocity error, which drives the voltage applied to the motors. Higher K values result in larger desired velocities, creating greater velocity errors and demanding increased motor voltages. Figure 8 highlights this relationship, showing that while higher K values improve responsiveness, they also lead to higher electrical loads on the motors. For $K = 100$, the voltage demand exceeds the maximum allowable 12V, making it unsuitable for implementation.

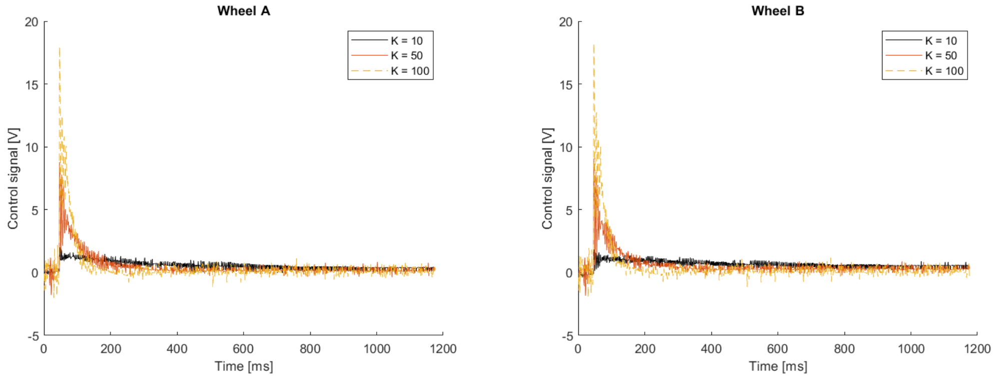

(a) Wheel A (b) Wheel B

Figure 7: Control signal for different values of K

Based on the analysis, $K = 50$ provides a suitable trade-off. It ensures a fast step response while maintaining compliance with the 12V voltage limitation. While theoretically, a very high K value would further accelerate convergence, practical considerations—most notably the voltage constraint—make such implementations impossible. Thus, $K = 50$ emerges as the optimal choice, balancing system performance and operational feasibility.

2c State Estimator and Controller with Pole Placement for Step Response

From Figure 8, it can be observed that when the closed-loop pole of the estimator is 10 times slower than that of the state feedback controller, the accuracy of the initial estimate has a significant impact on system performance.

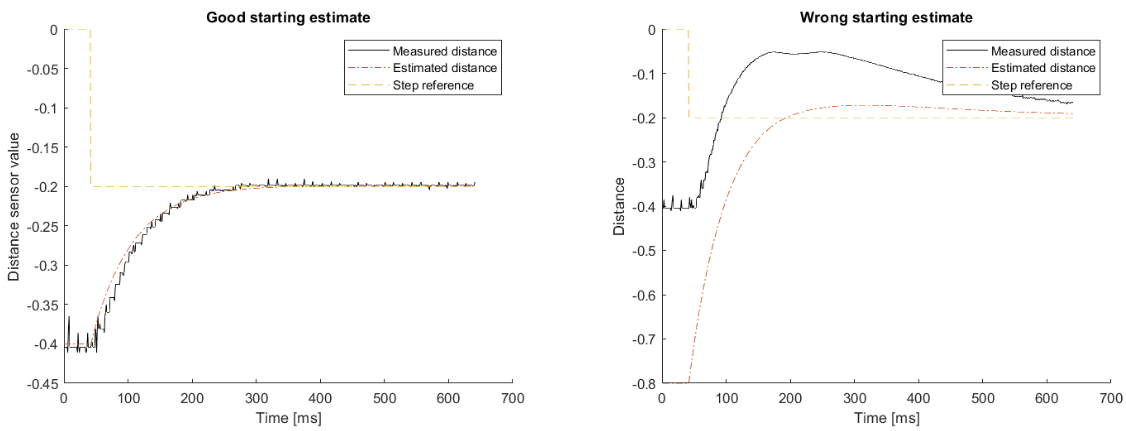

(a) Good position estimate (b) Bad position estimate

Figure 8: Measured and estimated distance when applying a step position reference

When the initial estimate is accurate, the estimated distance closely matches the measured distance, enabling the cart to promptly and accurately reach the desired step reference. Conversely, if the initial estimate is poor, the slower estimator poles, which are 10 times slower than the state feedback controller poles ($L = -0.0046$), reduce the estimation's ability to converge quickly to the measured distance. As a result of this slow convergence, the system fails to reliably determine the cart's position. This leads to an initial overshoot of the desired step response. Only after a delay, as the estimated and measured distances gradually align, does the measured distance approach the step reference. Consequently, the control performance is unsatisfactory except in cases where the initial estimate is accurate.

Both scenarios, however, demonstrate relatively consistent behavior in the estimator. This consistency may be attributed to the slower estimator poles, which reduce the estimator's response speed. While this slower response limits the system's ability to quickly adapt, it also enhances robustness against noise.

If the closed-loop poles could be freely chosen, we would recommend setting the estimator poles to be four times faster than the state feedback controller poles. When the estimator poles p_e are set to be four times faster than the controller pole p_c, they are calculated as:

$$p_c = e^{-\sigma \cdot T_s} \approx 0.955 \qquad \text{with:} \quad \sigma = \frac{4.6}{t_s} \tag{14}$$

$$p_e = e^{T_s \cdot p_c \cdot 4} \approx 0.998 \tag{15}$$

This configuration would achieve a faster estimator response while maintaining reasonable robustness to measurement noise, striking a balance between speed and noise sensitivity.

In conclusion, the results of this experiment highlight the critical importance of ensuring that the estimator poles are faster than the controller poles. This requirement arises from the controller's dependency on precise and timely estimates to function effectively.